



# Vascular imaging in renal donors

Ayaz Aghayev, Sumit Gupta, Borna E. Dabiri, Michael L. Steigner

Cardiovascular Imaging Program, Departments of Radiology, Brigham and Women's Hospital and Harvard Medical School, Boston, MA 02115, USA

*Contributions:* (I) Conception and design: A Aghayev; (II) Administrative support: A Aghayev, M Steigner; (III) Provision of study materials or patients: A Aghayev, M Steigner; (IV) Collection and assembly of data: A Aghayev, S Gupta, B Dabiri; (V) Data analysis and interpretation: None; (VI) Manuscript writing: All authors; (VII) Final approval of manuscript: All authors.

*Correspondence to:* Ayaz Aghayev, MD. Cardiovascular Imaging Program, Department of Radiology, Brigham and Women's Hospital, Harvard Medical School, Boston, MA, 75 Francis Street, Boston, MA 02115, USA. Email: aaghayev@bwh.harvard.edu.

**Abstract:** Imaging plays a crucial role in pre-transplant evaluation to enhance the probability of a successful outcome. Its aim is to define kidney and vascular anatomy and to assess potential pathologies. Each modality has advantages and disadvantages. Computed tomography angiography (CTA) is the most commonly used imaging modality, however, magnetic resonance angiography (MRA) can be used in selected cases. The purpose of this review article is to provide an overview of available imaging modalities, their benefits, risks, advantages, and disadvantages. Imaging findings that indicate particular anomalies and pathologies that may affect living renal donor selection will be discussed.

**Keywords:** Renal donor; transplantation; vascular imaging

Submitted Aug 20, 2018. Accepted for publication Nov 08, 2018.

doi: 10.21037/cdt.2018.11.02

View this article at: <http://dx.doi.org/10.21037/cdt.2018.11.02>

## Introduction

The prevalence of end-stage renal disease (ESRD) is increasing throughout the world, posing a significant challenge for health care systems worldwide (1). Renal transplantation is considered the treatment of choice for ESRD, and successful kidney transplantation can be expected to significantly increase a patient's quality of life. The lack of cadaveric organ availability has led to transplantation from living donors. In order to decrease the gap between the demand for and availability of kidneys from healthy young people, organs from an older population with comorbidities has increased in recent years (1). Harvesting kidneys, especially from less ideal donors, requires especially careful preoperative assessment to minimize the donor's risk of complications. Further, due to a rapid increase in the use of laparoscopic surgical techniques and the associated limited operative field of view, a precise delineation of the anatomy is required prior to the intervention (2). As visualization of the posterior and medial superior aspects of the kidneys and the renal veins

are limited during laparoscopic surgery (3), imaging plays a fundamental role in the non-invasive evaluation of the kidneys and vasculature. Non-invasive imaging modalities, such as Doppler ultrasound, multiphase computed tomography (CT) including CT Angiography (CTA), and magnetic resonance imaging (MRI) or angiography (MRA) are available options post-processing following image acquisition.

## Living renal donor evaluation

All living donors should have a detailed medical evaluation to ensure donor's safety: an extensive history, physical exam, blood and urine screening tests, electrocardiogram, chest X-ray, and imaging evaluation of kidney anatomy and its associated vasculature (4). Most commonly, CTA, which has been demonstrated as an accurate, safe, and cost-effective technique, is performed for anatomical evaluation of the renal donor (5,6). Some centers use MRI/MRA in selected living renal donor patients (7). Ultrasound is less frequently used in living donor kidney evaluations. A common

**Table 1** Living donor evaluation

History
Hypertension
Diabetes
Intravenous drug abuse
Infections
Medication use
Cardiovascular diseases
Cancer history
Autoimmune disease history
Physical exam
Weight/Height
Blood pressure
General physical exam
Lymph node examination
Breast exam (female patients)
Prostate exam (older males)
Laboratory
CBC
Coagulation screen
Creatinine clearance
GFR measurements
Urinalysis
Liver panel
Electrolytes
Antiviral screening
PPD
Electrocardiogram
Chest X-ray
PAP
Anatomic evaluation of the kidneys
CTA or MRA

indication for ultrasound is for screening patients with a family history of autosomal dominant polycystic kidney disease (8). The use of catheter angiography has declined significantly with the rapid advance of cross-sectional techniques. In this review, we concentrate primarily on

CTA and MRA modalities since ultrasound and catheter angiography play very small roles in current renal donor anatomy assessment protocols. *Table 1* lists the tests that may be used for renal donor evaluation.

### CTA versus MRA in living renal donor evaluation

The main goal of imaging is capturing the anatomical detail of the kidneys, vasculature, and associated or incidental pathologies. Multiphase, high-resolution image acquisition with CTA or MRA can provide detailed evaluation of the kidneys. Each modality has its advantages and disadvantages. Small studies have shown that CT and MRI are comparable techniques for living donor evaluation (9-11). A pilot study with a 3.0 Tesla MRI for kidney anatomy assessment demonstrated high sensitivity (96%) for delineating arterial anatomy, but lower sensitivity (76%) for venous anatomy (6). Another small study demonstrated that non-contrast MRI could also be a potential replacement for CTA (12). The main advantage of MRI/MRA is that it is a radiation-free imaging modality and can be used for patients with an iodine allergy (13). The limitations of MRI are the spatial resolution and small coverage per slab in a single acquisition, which potentially may result in missing the small accessory arteries arising from pelvic vessels (14). Other potential issues with MRI are motion artifact due to breathing in longer sequences and poor coordination between the injection of the contrast material and image acquisition (7). Further, small stones and calcifications can easily be missed on MRI images, possibly necessitating additional imaging (13).

Improvements in CTA have resulted in superb spatial resolution with shorter scan periods, which can substantially reduce motion artifact. Prospective studies with larger populations have shown that CTA is more accurate than MRA for renal donor evaluation (15,16). Liefeldt *et al.* demonstrated that CTA shows more accessory renal arteries than MRA (15). Therefore, CTA is still preferred and is the gold standard despite theoretical risks of nephrotoxicity and radiation (7). Notably, recent studies have clearly stated that iodinated contrast agents are not nephrotoxic in patients with normal kidney function (eGFR of 45 mL/min/1.73 m<sup>2</sup> or higher) (16). Adjustments of the radiation protocol and several other techniques have been studied, including iterative reconstruction or lowering the tube voltage (17,18). Davarpanah *et al.* reduced tube voltage current from 120 to 80 kV resulting in a significant reduction of radiation that also improved the signal-to-noise ratio (SNR) and

**Table 2** Main advantage and disadvantages of the imaging modalities

Modality	Advantages	Disadvantages
Ultrasound	Widely available; ideal for screening	Operator dependent; difficult to assess vessel anatomy; time consuming
Angiography	Excellent resolution of arterial anatomy	Invasive procedure; radiation; iodine contrast agent associated nephrotoxicity or allergy; limited to vascular anatomy
CT/CTA	Superb spatial resolution for small vessels; multiphase acquisition for vessels, parenchyma and collecting system evaluation	Radiation; iodine contrast agent associated nephrotoxicity or allergy
MRI/MRA	No radiation; multiphase acquisition for vessels, parenchyma and collecting system; excellent tissue characterization	Expensive; low spatial resolution for small vessels; gadolinium contrast agent associated Nephrogenic Systemic Fibrosis, or allergy

contrast to noise ratio (CNR) (17). Recently, there has been a rapid increase in the use of dual-energy CT (DECT) in renal imaging (19), particularly in renal mass evaluation, in which DECT can create virtual non-enhanced data sets and minimize image acquisition in the classic triple phase protocol. DECT can potentially be applied to the renal donor imaging protocol and can be expected to aid in further minimizing radiation dose. *Table 2* summarizes the advantages and disadvantages the different imaging modalities.

An important consideration in any screening study is its capacity to generate more imaging follow up for characterizing incidental findings. However, multiphase imaging of the abdomen and pelvis can aid in identifying pathologies in the renal donor population. A study by Tan *et al.* demonstrated that in a cohort of 1,597 patients, 95.4% of the incidental findings could be characterized on multiphase CT imaging, and only 4.5% of the findings warranted additional workup (20).

### CTA protocol in renal donor evaluation

CTA imaging for healthy donors can be performed as a 4-phase CT image acquisition protocol (21). The initial phase should be non-contrast image acquisition, followed by arterial phase CTA, nephrographic phase (100 s delay), and excretory phase (pyelographic phase). The detailed protocol of the scan is shown in *Table 3*.

#### Non-contrast image acquisition

The non-contrast phase is acquired following the topogram and is the ideal phase for evaluating the presence of potential stones and calcifications in the kidneys (*Figure 1*). However, some centers advocate excluding the non-contrast

phase because these are healthy patients and the arterial phase is sufficient for visualizing kidney stones (22,23). However, this may increase false-positive “stone” detection on CT studies.

#### Arterial phase CTA image acquisition

CTA for renal donors can be performed with automated bolus tracking, similar to regular CT angiography studies that assess abdominal arterial anatomy (21). Nonionic contrast agent with a concentration of 300 or 370 mg iodine/mL can be administered with an injection rate of 4 to 5 mL/s. The maximum contrast dose should be 100 or 120 mL based on iodine concentration. The ideal anatomic coverage for CTA should extend between the dome of the diaphragm and the distal portion of the common iliac arteries or iliac crest (24). An additional option for obtaining the CTA is a slightly delayed arterial phase image acquisition that can be done with a 25 to 30 s delay (23,25). With delayed arterial phase imaging, some venous structures, including the adrenal and gonadal veins, can be evaluated.

#### Nephrographic phase image acquisition

The nephrographic phase, performed at ~100 s, is ideal for renal parenchymal evaluation, particularly for small renal masses (26,27) (*Figure 2*). This phase can accurately depict venous anatomy of the donor’s kidneys, particularly small veins such as the adrenal and gonadal veins (27).

#### Excretory phase image acquisition

The excretory or pyelographic phase is usually obtained

**Table 3** CTA protocol for renal donor evaluation

Phase	Scan range and reconstruction
Topogram	Abdomen and pelvis
Precontrast	From the dome of the diaphragm to the iliac crest Axial thin images reconstruction (thickness × interval): 1 mm × 0.8 mm Axial/coronal/Sagittal reconstruction (thickness × interval): 3 mm × 3 mm
Monitoring	ROI at the level of celiac artery
Arterial	From the dome of the diaphragm to the iliac crest
Bolus tracking injection rate of 5 mL/s total dose 100 mL contrast	Axial thin images reconstruction (thickness × interval): 1 mm × 0.8 mm Axial/coronal/sagittal reconstruction (thickness × interval): 3 mm × 3 mm Axial/coronal MIP reconstruction (thickness × interval): 8 mm × 2 mm
Nephrogram	From the dome of the diaphragm to the iliac crest
100-second delay	Axial thin images reconstruction (thickness × interval): 1 mm × 0.8 mm Axial/coronal/sagittal reconstruction (thickness × interval): 3 mm × 3 mm
Excretory (pyelographic)	Abdomen and pelvis
6 minutes delay	Axial thin images (thickness × interval): 1 mm × 0.8 mm Axial/coronal/sagittal reconstruction (thickness × interval): 3 mm × 3 mm

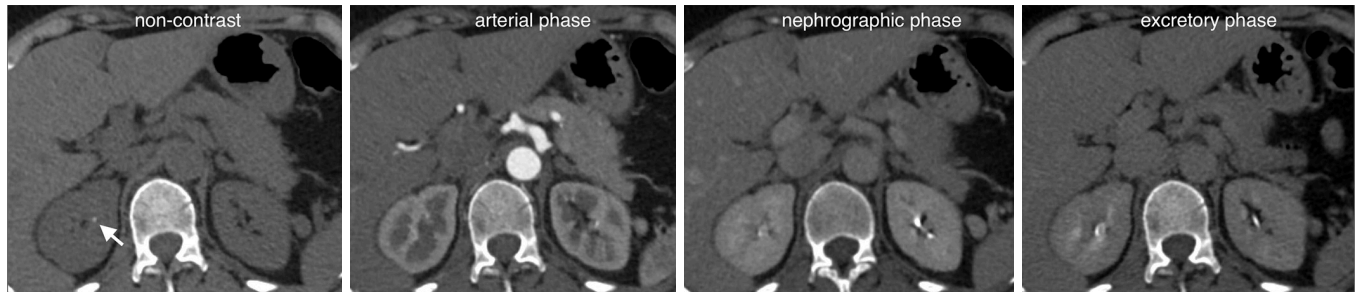


**Figure 1** Four-phase CT images demonstrate a tiny stone in the right kidney upper pole (arrow), which is not appreciated on arterial, nephrographic or excretory phases.

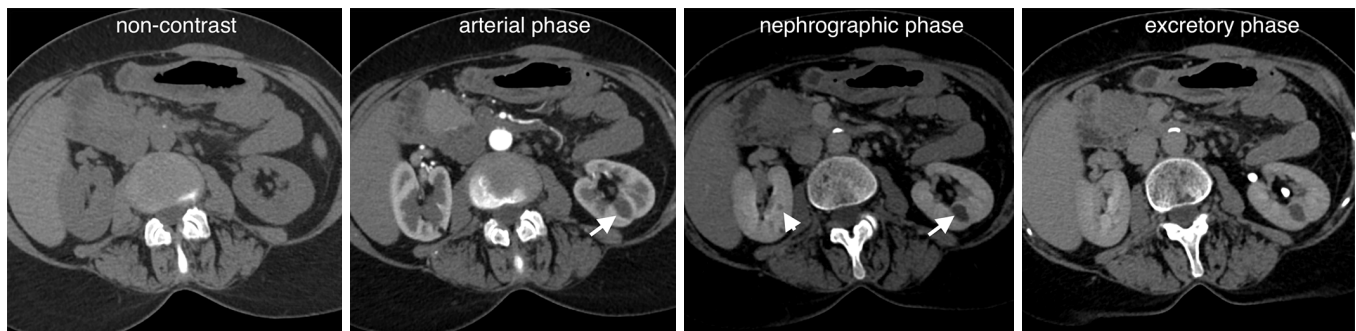


**Figure 2** Four-phase CT images show an 8 mm cyst in the left kidney (arrow), which is best appreciated in the nephrographic phase. On arterial phase only, the image it can be masked by the nonenhanced medulla. A tiny cyst (arrowhead) in the right kidney is also well-seen on nephrographic phase.

**Table 4** MRA protocol for renal donor evaluation

Phase	Scan and reconstruction
Localizer	Abdomen and pelvis
Pre-contrast	From the dome of the diaphragm to the iliac crest: coronal T2 (e.g., HASTE): slice thickness 5 mm; axial T1 (e.g., FLARE): slice thickness 5 mm; in and out phase, diffusion weighted imaging
Monitoring	ROI in descending thoracic aorta
Arterial	From the dome of the diaphragm to the iliac crest
Bolus tracking: injection rate of 2 mL/s of gadolinium agent	Coronal 3D-spoiled GRE (e.g., TWIST, VIBE): slice thickness 1.5–3.0 mm
Non-contrast MRA	Coronal SSFP (e.g., TruFISP): slice thickness 1.5–3.0 mm
Nephrogram	From the dome of the diaphragm to the iliac crest
100 second delay	Coronal 3D-spoiled GRE (e.g., TWIST, VIBE): slice thickness 1.5–3.0 mm
Excretory (pyelographic)	Abdomen and pelvis
10 minutes delay	Coronal 3D-spoiled GRE (e.g., TWIST, VIBE) or Coronal SSFP (e.g., TruFISP) for non-contrast exams: slice thickness 1.5–3.0 mm

between four to eight minutes following initial contrast administration. In the authors' institution, the fixed time period for image acquisition following the contrast injection is 6 minutes. During the excretory phase, the anatomy of the collecting system and urothelial pathologies can be imaged. In order to reduce the radiation dose, some centers obtain a scout image only (28). However, given the advancing age of renal donor patients, urothelial masses or lesions can be missed if only a scout is obtained.

### MRA protocol in renal donor evaluation

Similar to CT imaging, multiphase MRI acquisition can be performed for renal donor imaging. Initial pre-contrast sequences include axial and coronal T2-weighted images, which can be used as the localizer and for visualization of potential masses, including cystic lesions within the kidney. Additional pre-contrast in-phase and out-of-phase sequences can be obtained to evaluate fatty masses within the kidneys. Other sequences, such as diffusion weighted imaging (DWI), can be obtained to aid in assessment of other incidental findings. Although MRI offers an excellent assessment of soft tissue lesions, CT is superior for the detection of small renal stones (6,29). For vascular assessment, post-contrast arterial (MRA) and subsequent venous phases (MRV) can be obtained using 3D fast-gradient echo sequences following the administration of an intravenous gadolinium agent. The excretory phase is typically obtained ten minutes following

contrast administration for evaluation of collecting systems and ureters. *Table 4* provides detailed protocol and list of sequences.

### Pre-contrast image acquisition

A variety of pre-contrast sequences can be used to aid in characterizing renal lesions and other incidental findings. These typically include a T2 sequence, such as coronal T2 HASTE (with and without fat saturation) (6). This sequence can identify cystic renal lesions, including simple cortical cysts and peripelvic and parapelvic cysts within the sinus. Additional axial T2 weighted imaging and axial T1 sequences, such as T1 FLARE with in and out of phase sequences, can be obtained so that cystic renal lesions and/or masses can be further characterized (11). Axial DWI can also be used to aid in further assessment of lesions. Several investigators have used non-contrast MRA techniques for vascular assessment so as to avoid administering an intravenous gadolinium agent. In such instances, non-contrast MRA, coronal B-SSFP, and axial B-SSFP sequences such as TruFISP have been performed (11). Although non-contrast MRA correlates well with 3D contrast-enhanced MRA for the evaluation of the renal artery, a study assessing renal artery stenosis reported that reader confidence was lower (30). However, with increasing advancement in MRI hardware and software, a study of 60 patients comparing non-contrast MRA to CTA showed that non-contrast MRA

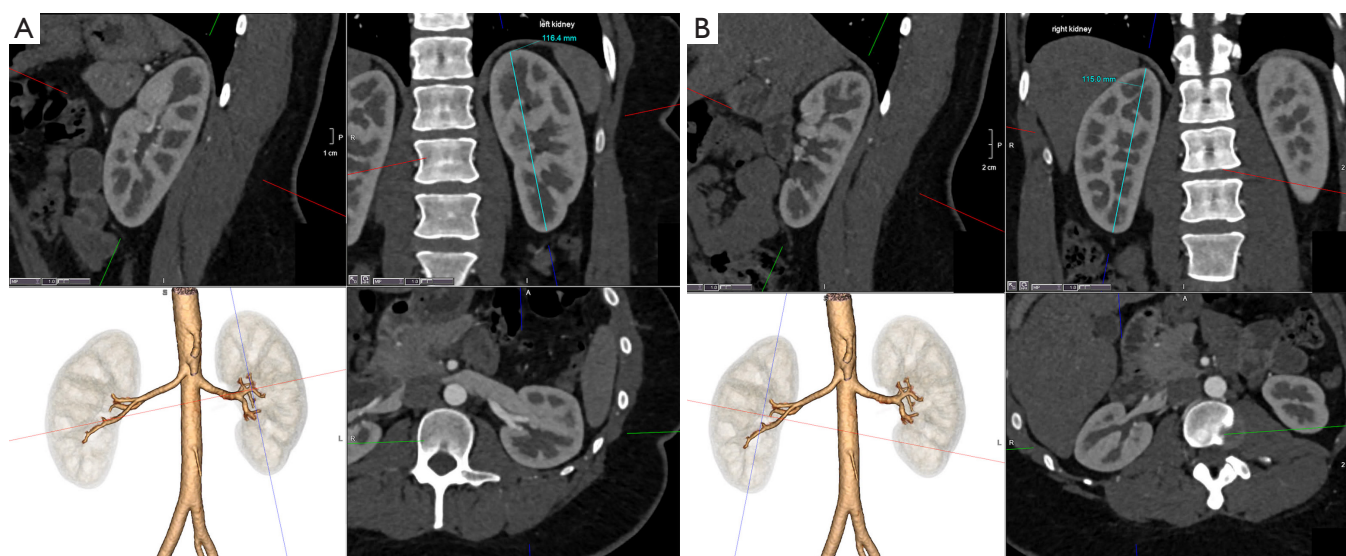


**Figure 3** The left (A) and the right (B) kidney measurements on multiplanar reformatted (MPR) CT images.

demonstrated comparable results in identifying renal artery and venous anatomy (11).

#### **Post-contrast MRA and MRV**

Contrast-enhanced sequences can be used to obtain information regarding arterial and venous anatomy and as an aid in providing an additional opportunity to characterize incidental lesions. Standard dosing or weight-based formulations such as 0.1 mL/kg intravenous gadolinium agents can be used with injection rates of 1.5–2 mL/s as is used in MRA and MRV applications (21). It should be noted that gadolinium-based contrast agents have no nephrotoxic events and are safe to use in those with glomerular filtration rates >30 mL/min (31). Common sequences include time-resolved coronal 3D-spoiled GRE sequences (21,32) or 3D-spoiled GRE sequences such as VIBE. Contrast-enhanced sequences are typically obtained with coronal slice thicknesses ranging between 1.5 and 3 mm for 3D post-processing. Bolus tracking within the descending thoracic aorta is used to trigger arterial phase imaging. Immediately following arterial phase imaging, pre-scanning and localization for venous phase imaging is begun and may take 30–60 s.

#### **Excretory phase**

Following venous phase imaging, a 10 minute-delay excretory phase imaging is obtained for optimal urothelial

opacification. To enhance urinary excretion, several protocols include oral ingestion of 500 mL of water 15 minutes prior to scanning and an additional 200 mL of intravenous saline following contrast administration (6).

#### **The role of post-processing and 3D reformatting in CTA and MRA**

Post-processing and 3D reformatting can generate an overall display of the anatomy and create a simulation of the renal anatomy for use by surgeons (23). Multiplanar reformatting (MPR), curved MPR (cMPR), Maximum Intensity Projection (MIP), and 3D volume rendered images are an essential part of renal donor imaging. Subsequent to raw data acquisition, thin slice volumetric axial reconstruction should be performed for all phases for postprocessing. In addition, thick slice reconstruction in an axial, coronal, and sagittal plane can be performed and sent to the picture archiving and communication system (PACS). For arterial phase data both in CTA and MRA, maximum intensity projection (MIP) image reconstruction will aid in identifying small tiny accessory vessels. Anatomy evaluation, as well as most of the measurements, should be performed on processed images. The initial step should be kidney measurements in the MRP images (Figure 3). Then 3D volume rendered renal arteries and measuring pre-hilar arterial branching distance on cMPR images is obtained (Figure 4). Small accessory renal arteries can be missed on regular axial images. A stack of MIP images

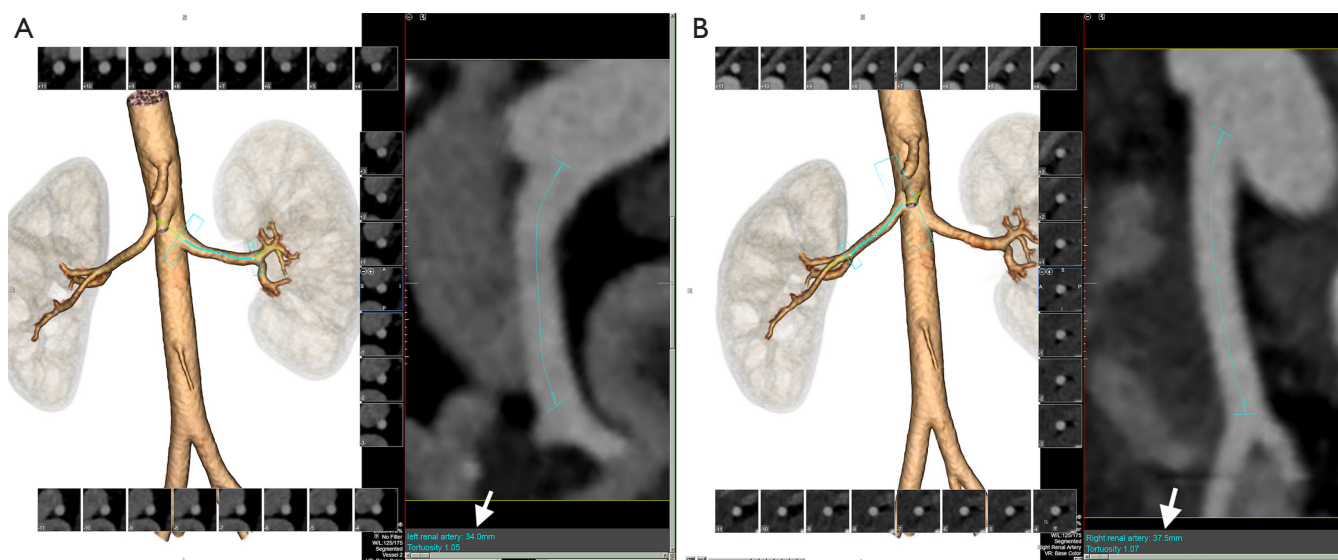


**Figure 4** The left (A) and the right (B) renal artery pre-hilar arterial branching measurements on curved multiplanar reformatted (cMPR) CT images. The arrows in the left lower corner demonstrate the distance to the branching.

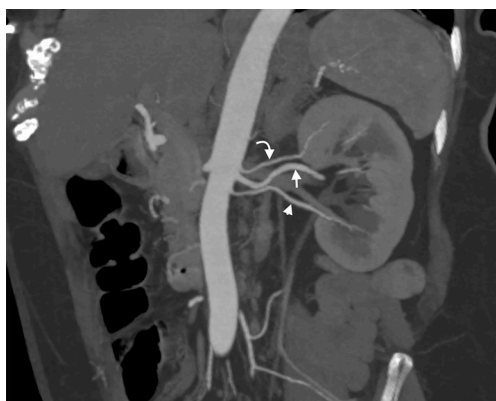


**Figure 5** Maximum intensity projection (MIP) CTA image through the kidney shows main (arrows) and small accessory (arrowhead) as well as aberrant renal (curved arrow) arteries.

through the kidneys in multiple planes can increase diagnostic confidence (33) (*Figure 5*). In addition to pre-hilar arterial branch measurements, some centers measure the distance between the right inferior vena cava (IVC) margin and the right artery bifurcation (3). Renal veins, as well as abnormal large venous drainage into the renal veins, should be evaluated on multiple planes, and the distance to the veins and confluences can be measured on the cMPR images (*Figure 6*). The final step is obtaining 3D volume rendered images from the excretory phase (*Figure 7*).

### Renal vascular variations, pathologies, and criteria for donor selection

The vascular anatomy is the key factor in donor kidney selection. Kidneys with less complex vascular anatomy and variations should be selected for transplantation when both kidneys are normal (23).

#### *Renal artery anatomy and variations*

Renal artery variations are not uncommon and are mainly classified into two groups: (I) early branching; and (II) extrarenal arteries (34). Early branching (a.k.a. perihilar branching) is considered as having occurred when the renal artery branches within 20 mm of its origin (*Figure 8*). Studies have shown that the incidence of early branching to be as high as 21% (35,36). For the right kidney, early branching is considered when the branching occurs behind the IVC (retrocaval branching), or within 1 cm of the IVC right margin (3). A second group, the extrarenal arteries, is vessels with a separate origin from the aorta and has a smaller caliber than the main renal artery (3). This group can be subclassified into accessory renal and aberrant renal arteries. The accessory renal arteries extend to the kidney through the hilum with the main renal artery (*Figure 9*) (34). Although most of the accessory renal arteries arise from the aorta, there are reported cases in which the origin can be from the iliac,



**Figure 6** Curved multiplanar reformatted (cMPR) CTA images of the venous system demonstrate distance to the left (A) and right (B) renal vein confluences as well as gonadal (C) and adrenal veins (D) drainages into the left renal vein. Arrows indicate gonadal vein in (C), adrenal gland vein in (D).

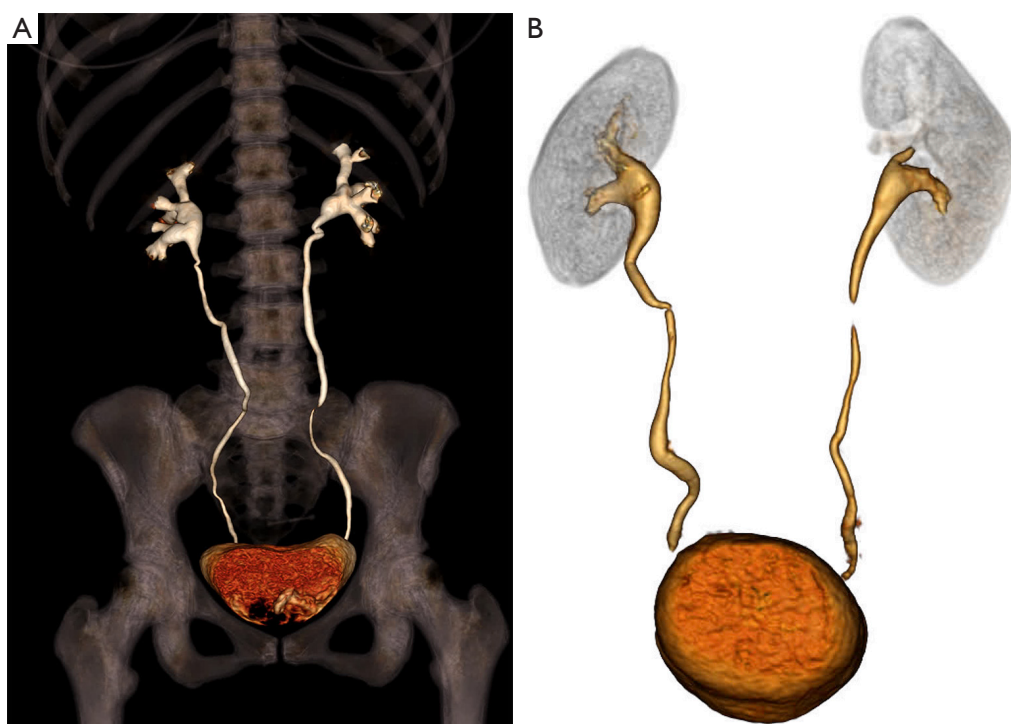


**Figure 7** Volume-rendered 3D CT (A) and MRI (B) excretory phase images demonstrate the normal anatomy of the collecting system.

gonadal, middle colic, mesenteric vasculature including superior, inferior mesenteric arteries, and from the contralateral kidney artery (3,37). The aberrant artery can be a polar or capsular artery, or a polar artery entering the kidney through the inferior or superior pole (Figure 10) (33,34). Capsular arteries are thin, hairline vessels coursing/entering tangentially to the renal capsule; sometimes it can be difficult to differentiate polar arteries from capsular arteries (3). The presence of more than two accessory renal arteries can be considered a possible

contraindication, given the high risk of thrombosis and increased operation time (Figure 11) (27). In particular, accessory arteries less than 3 mm in diameter present technical difficulties and have resulted in a high rate of thrombosis (38). In certain situations, small polar or capsular arteries—a diameter of less than 2 mm—can be satisfactory as the infarcted kidney tissue volume will be less than ten percent (39). Nevertheless, sacrificing lower polar renal arteries (even smaller, less than 2 mm, vessels) is contraindicated as they are associated with

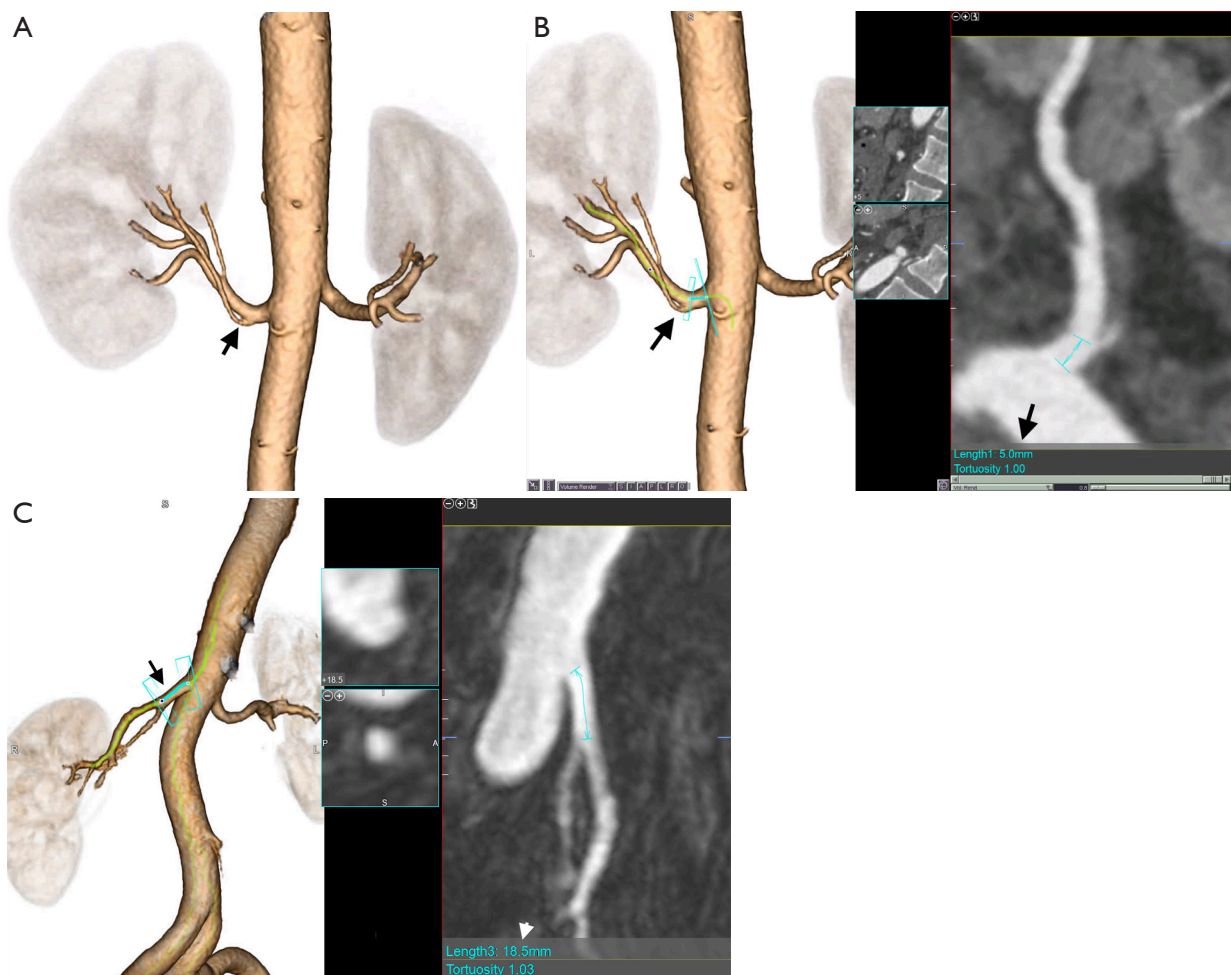


**Figure 8** Volume-rendered 3D CTA image of the abdominal aorta and renal arteries (A) shows early branching (arrow) of the left renal artery, and curved multiplanar reformatted (cMPR) image of the same artery (B) demonstrates the distance (arrows) from the aorta to the level of the branching. Similarly, volume-rendered 3D MRA image of the abdominal aorta and right renal artery (C) demonstrate early branching (black and white arrows), and CTA and MRA images are comparable.

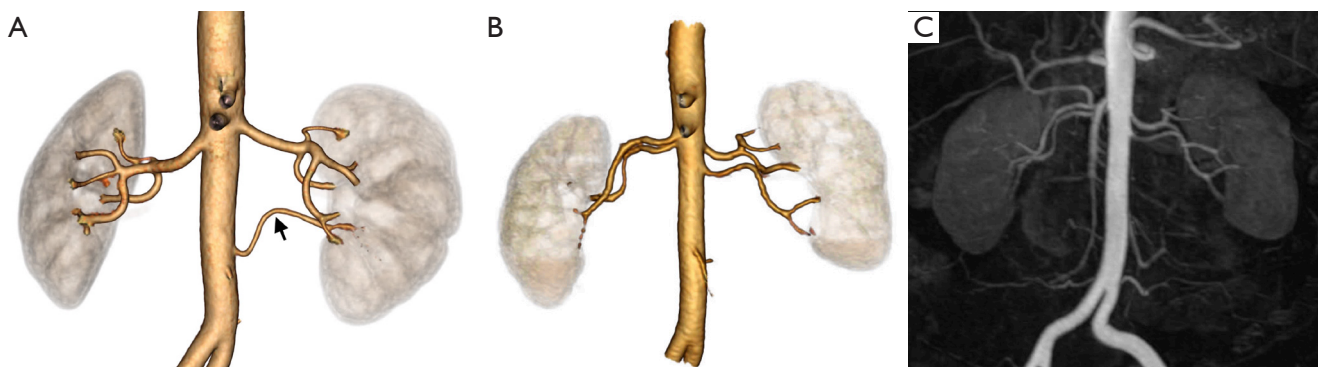


**Figure 9** Small accessory left renal artery (arrow) is seen in the volume-rendered 3D CTA image (A). Similarly, in a volume-rendered 3D (B) and maximum intensity projection (MIP) (C) MRA images demonstrate bilateral accessory renal arteries.

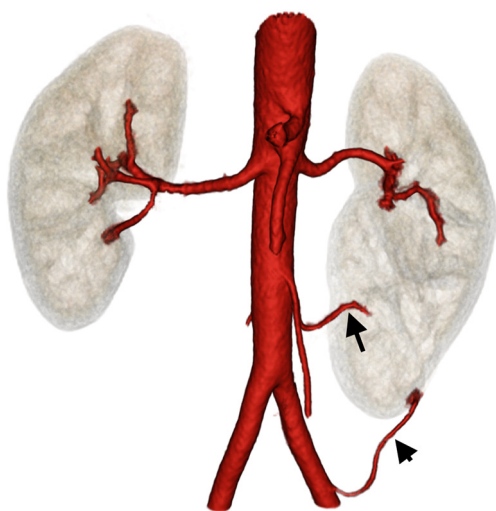


**Figure 10** Volume-rendered 3D CTA image shows two aberrant (polar) renal arteries supplying the left kidney one is arising from the aorta (arrow), and the second one is originating from the left common iliac artery (arrowhead).

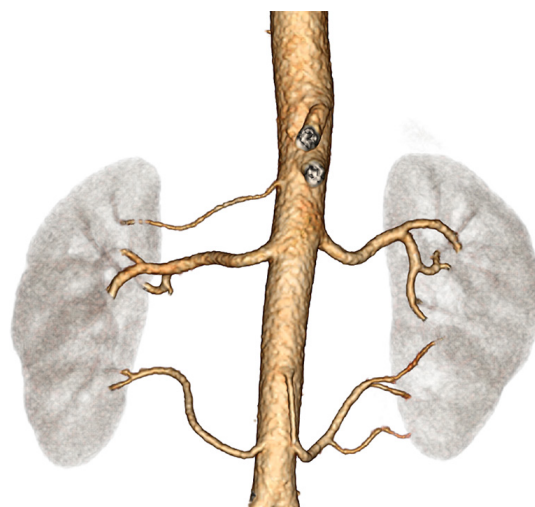


**Figure 11** A patient excluded from the renal donor list due to three right renal arteries, and two left renal arteries.

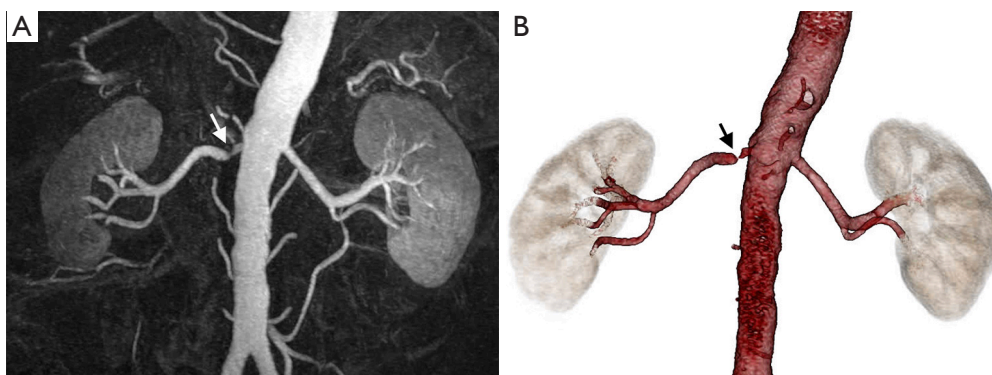


**Figure 12** Maximum intensity projection (MIP) (A) and volume-rendered 3D (B) MRA images demonstrate severe stenosis (arrows) at the proximal segment of the right renal artery due to atherosclerotic disease.

a higher rate of recipient ureteral complications such as pyeloureteral necrosis as these vessels supply upper urinary tracts (40).

### ***Renal artery pathologies***

Renal artery pathologies, such as fibromuscular dysplasia (FMD) or severe atherosclerotic disease, particularly in older patients, can be easily evaluated with imaging and may exclude patients from becoming donors (41,42). Renal arteries with sufficiently significant atherosclerotic disease may require intraoperative endarterectomy (38).

The amount and extent of calcified plaques in the renal artery should be reported as they can cause lacerations in the aorta and renal arteries during the surgery (3). Patients with FMD involving both renal arteries are not eligible to become donors; however, unilateral renal artery involvement can be considered in selective cases (*Figure 12*) (43,44).

### ***Renal vein variations and pathology***

Renal vein evaluation is extremely important, for two reasons. First, venous bleeding is the most common



**Figure 13** Volume-rendered 3D (A) and maximum intensity projection (MIP) (B) CTA images demonstrate incidentally detected fibromuscular dysplasia (FMD) both renal arteries (arrows). Similarly, a patient with incidentally detected FMD on MIP MRA image (C) and was confirmed on conventional angiography image (D). Arrows in (C) indicates FMD in the right renal artery.



**Figure 14** Maximum intensity projection (MIP) CTA image (A) demonstrates a circumaortic left renal vein; the branch anterior to the abdominal aorta (arrow) is draining into the proximal portion of the inferior vena cava (IVC), whereas the branch posterior to the abdominal aorta (arrowhead) is draining to the distal portion of the IVC. MIP CTA image demonstrates retroaortic left renal vein (arrow) (B).

reason for the conversion of laparoscopic to open surgery; therefore, it requires a more detailed presurgical evaluation (45). Second, the anatomic variance of the renal veins is more common than a renal artery, and the left renal vein has a higher proportion of all venous variance (7,25,46). The most common left renal vein variations are the supernumerary (accessory) renal vein and circumaortic left renal vein: 15–30% and 8–11%, respectively (Figure 13) (24,28). A retroaortic left renal vein is a relatively less common anatomic variance with a reported incidence of approximately three percent (Figure 14) (24). During the left renal vein evaluation, large systemic tributaries draining into the left renal vein, including gonadal, adrenal, lumbar, and dilated retroperitoneal veins, should be carefully delineated (35). Duplicate or multiple renal vein drainages are commonly seen in the right kidney (47). It has been shown that multiple renal veins are associated with a higher incidence of vein thrombosis following transplantation, and

therefore, these kidneys are considered a contraindication for transplant. One of the main rationales for selecting the left kidney is the presence of a long segment of left renal vein, permitting surgeons easy anastomosis. However, a randomized European trial of hand assisted donor nephrectomy demonstrated that operating time for right-sided nephrectomy is actually shorter than that of a left sided one (48). There was no difference between left and right-sided donor nephrectomy in complication rates or graft survival. In addition, venous anomalies associated with the inferior vena cava (IVC) should be evaluated in detail (Figure 15).

#### *Incidental findings*

Imaging can incidentally detect pathologies such as a stone, neoplastic masses, polycystic kidney disease, or hydronephrosis. Kidneys with tiny single stones (<5 mm)

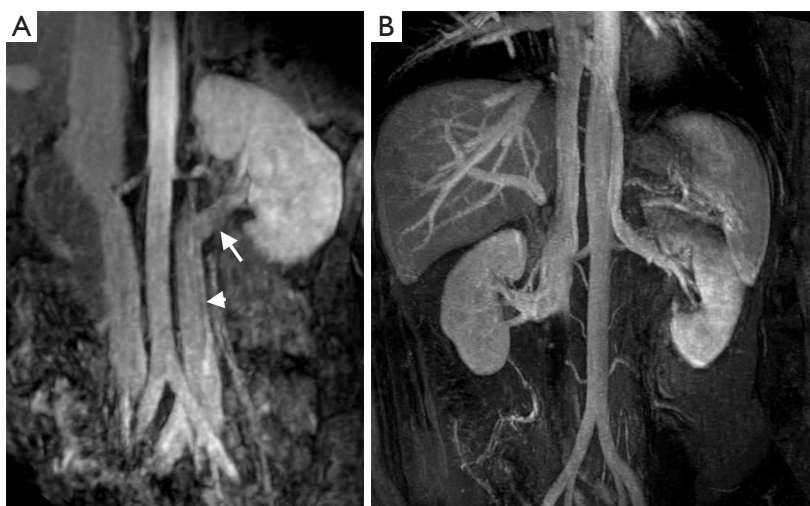


**Figure 15** Maximum intensity projection (MIP) MRA image (A) demonstrate duplicated IVC and the left renal vein (arrow) is draining into the left-sided IVC (arrowhead). Coronal MIP MRA image (B) demonstrates rare venous anomaly of the azygous continuation of IVC, and left renal vein is draining into the azygous at the level of the heart.

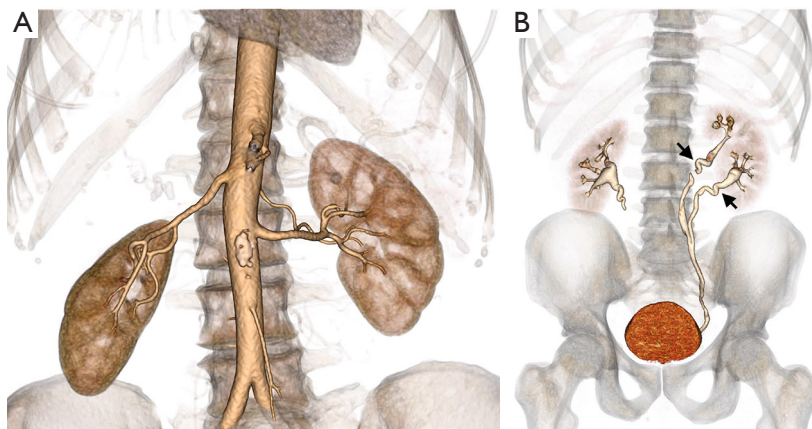


**Figure 16** Volume-rendered 3D CT image (A) shows a slightly ptotic right kidney. Volume-rendered 3D CT image (B) demonstrates partial duplex collecting system on the left (arrows), and fuses at the level of the midabdomen.

or small cysts (<5 mm) are not a contraindication and can be used for transplantation (49,50). An *ex-vivo* ureteroscopy technique has been safely used to remove larger or multiple stones from the kidneys and render these organs eligible for transplant (51). However, an additional workup may be required for large or multiple stones so as to exclude underlying hereditary or systemic disorders. Small, benign renal masses (<5 mm), such as renal angiomyolipoma, are not a contraindication for surgery, and larger (>5 mm) masses can be locally excised intraoperatively prior to the transplantation (52,53). Not all of the kidneys with developmental and collecting system anomalies, including

complete or partial ureteral duplication and ureteropelvic junction obstruction, should exclude one from being a donor (Figure 16). However, patients with horseshoe kidneys and renal agenesis are not eligible for the procedure (Figure 17).

### Summary

Transplantation remains the best option for patients with end-stage renal disease. Detailed pre-transplant assessment of the donor's kidney is extremely important for both the donor and recipient. Although there are a several imaging

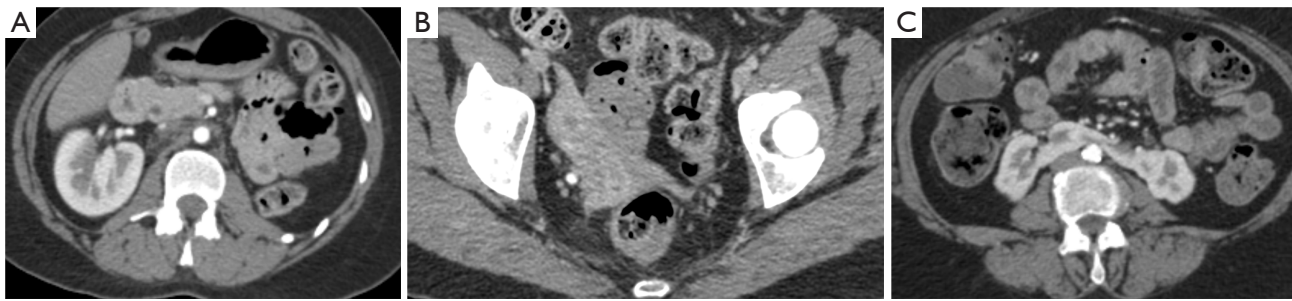


**Figure 17** Axial CT image through the abdomen (A) demonstrates the congenital absence of the left kidney with a unicornuate uterus (B), and a CT image through the abdomen (C) in another patient shows a horseshoe kidney.

modalities available, currently CTA remains the preferred and gold standard imaging modality despite theoretical risks of radiation and nephrotoxicity. Post-processing and 3D reformatting are crucial elements in renal donor evaluation and measurements.

### Acknowledgments

None.

### Footnote

*Conflicts of Interest:* The authors have no conflicts of interest to declare.

### References

1. Tullius SG, Rabb H. Improving the Supply and Quality of Deceased-Donor Organs for Transplantation. *N Engl J Med* 2018;378:1920-9.
2. Simforoosh N, Basiri A, Tabibi A, et al. Comparison of laparoscopic and open donor nephrectomy: a randomized controlled trial. *BJU International* 2005;95:851-5.
3. Sebastià C, Peri L, Salvador R, et al. Multidetector CT of living renal donors: lessons learned from surgeons. *Radiographics* 2010;30:1875-90.
4. Davis CL, Delmonico FL. Living-donor kidney transplantation: a review of the current practices for the live donor. *J Am Soc Nephrol* 2005;16:2098-110.
5. Smith D, Chudgar A, Daly B, et al. Evaluation of potential renal transplant recipients with computed tomography angiography. *Arch Surg* 2012;147:1114-22.
6. Gulati M, Dermendjian H, Gomez AM, et al. 3.0Tesla magnetic resonance angiography (MRA) for comprehensive renal evaluation of living renal donors: pilot study with computerized tomography angiography (CTA) comparison. *Clin Imaging* 2016;40:370-7.
7. Harmath CB, Wood CG, 3rd, Berggruen SM, et al. Renal Pretransplantation Work-up, Donor, Recipient, Surgical Techniques. *Radiol Clin North Am* 2016;54:217-34.
8. Rankin SC, Jan W, Koffman CG. Noninvasive imaging of living related kidney donors: evaluation with CT angiography and gadolinium-enhanced MR angiography. *AJR Am J Roentgenol* 2001;177:349-55.
9. Moritz M, Halpern E, Mitchell D, et al. Comparison of CT and MR angiography for evaluation of living renal donors. *Transplant Proc* 2001;33:831-2.
10. Gluecker TM, Mayr M, Schwarz J, et al. Comparison of CT angiography with MR angiography in the preoperative assessment of living kidney donors. *Transplantation* 2008;86:1249-56.
11. Blankholm AD, Pedersen BG, Ostrat EO, et al. Noncontrast-Enhanced Magnetic Resonance Versus Computed Tomography Angiography in Preoperative Evaluation of Potential Living Renal Donors. *Acad Radiol* 2015;22:1368-75.
12. Israel GM, Lee VS, Edye M, et al. Comprehensive MR imaging in the preoperative evaluation of living donor candidates for laparoscopic nephrectomy: initial experience. *Radiology* 2002;225:427-32.
13. Neimatallah MA, Dong Q, Schoenberg SO, et al. Magnetic resonance imaging in renal transplantation. *J Magn Reson Imaging* 1999;10:357-68.
14. Bhatti AA, Chugtai A, Haslam P, et al. Prospective study comparing three-dimensional computed tomography and magnetic resonance imaging for evaluating the renal vascular anatomy in potential living renal donors. *BJU Int* 2005;96:1105-8.
15. Liefeldt L, Kluner C, Glander P, et al. Non-invasive imaging of living kidney donors: intraindividual

- comparison of multislice computed tomography angiography with magnetic resonance angiography. *Clin Transplant* 2012;26:E412-7.
16. Davenport MS, Khalatbari S, Cohan RH, et al. Contrast material-induced nephrotoxicity and intravenous low-osmolality iodinated contrast material: risk stratification by using estimated glomerular filtration rate. *Radiology* 2013;268:719-28.
  17. Davarpanah AH, Pahade JK, Cornfeld D, et al. CT angiography in potential living kidney donors: 80 kVp versus 120 kVp. *AJR Am J Roentgenol* 2013;201:W753-60.
  18. Singh AK, Sahani DV, Kagay CR, et al. Semiautomated MIP images created directly on 16-section multidetector CT console for evaluation of living renal donors. *Radiology* 2007;244:583-90.
  19. Kahn J, Grupp U, Rotzinger R, et al. CT for evaluation of potential renal donors - how does iterative reconstruction influence image quality and dose? *Eur J Radiol* 2014;83:1332-6.
  20. Tan N, Charoensak A, Ajwichai K, et al. Prevalence of incidental findings on abdominal computed tomography angiograms on prospective renal donors. *Transplantation* 2015;99:1203-7.
  21. Murphy DJ, Aghayev A, Steigner ML. Vascular CT and MRI: a practical guide to imaging protocols. *Insights Imaging* 2018;9:215-36.
  22. Singh AK, Sahani DV. Imaging of the renal donor and transplant recipient. *Radiol Clin North Am* 2008;46:79-93, vi.
  23. Hazirovan T, Oz M, Turkbey B, et al. CT angiography of the renal arteries and veins: normal anatomy and variants. *Diagn Interv Radiol* 2011;17:67-73.
  24. Kawamoto S, Montgomery RA, Lawler LP, et al. Multi-detector row CT evaluation of living renal donors prior to laparoscopic nephrectomy. *Radiographics* 2004;24:453-66.
  25. Wolin EA, Hartman DS, Olson JR. Nephrographic and pyelographic analysis of CT urography: principles, patterns, and pathophysiology. *AJR Am J Roentgenol* 2013;200:1210-4.
  26. Vernuccio F, Gondalia R, Churchill S, et al. CT evaluation of the renal donor and recipient. *Abdom Radiol (NY)* 2018;43:2574-88.
  27. Liu PS, Platt JF. CT angiography of the renal circulation. *Radiol Clin North Am* 2010;48:347-65, viii-ix.
  28. Graser A, Johnson TR, Hecht EM, et al. Dual-energy CT in patients suspected of having renal masses: can virtual nonenhanced images replace true nonenhanced images? *Radiology* 2009;252:433-40.
  29. Winchester P, Kapur S, Prince MR. Noninvasive imaging of living kidney donors. *Transplantation* 2008;86:1168-9.
  30. Glockner JF, Takahashi N, Kawashima A, et al. Non-contrast renal artery MRA using an inflow inversion recovery steady state free precession technique (Inhance): comparison with 3D contrast-enhanced MRA. *J Magn Reson Imaging* 2010;31:1411-8.
  31. Thomsen HS, Morcos SK, Almen T, et al. Nephrogenic systemic fibrosis and gadolinium-based contrast media: updated ESUR Contrast Medium Safety Committee guidelines. *Eur Radiol* 2013;23:307-18.
  32. Hussain SM, Kock MC, IJzermans JN, et al. MR imaging: a "one-stop shop" modality for preoperative evaluation of potential living kidney donors. *Radiographics* 2003;23:505-20.
  33. Ozkan U, Oguzkurt L, Tercan F, et al. Renal artery origins and variations: angiographic evaluation of 855 consecutive patients. *Diagn Interv Radiol* 2006;12:183-6.
  34. Holden A, Smith A, Dukes P, et al. Assessment of 100 live potential renal donors for laparoscopic nephrectomy with multi-detector row helical CT. *Radiology* 2005;237:973-80.
  35. Raman SS, Pojchamarnwiputh S, Muangsomboon K, et al. Surgically relevant normal and variant renal parenchymal and vascular anatomy in preoperative 16-MDCT evaluation of potential laparoscopic renal donors. *AJR Am J Roentgenol* 2007;188:105-14.
  36. Pozniak MA, Balison DJ, Lee FT Jr, et al. CT angiography of potential renal transplant donors. *Radiographics* 1998;18:565-87.
  37. Roth CG, Mizrahi DJ, Needleman L. Radiology of Kidney Transplantation. In: Ramirez C, McCauley J. editors. *Contemporary Kidney Transplantation. Organ and Tissue Transplantation*. Cham: Springer, 2018:249-91.
  38. Satyapal KS, Haffejee AA, Singh B, et al. Additional renal arteries: incidence and morphometry. *Surg Radiol Anat* 2001;23:33-8.
  39. Kok NF, Dols LF, Hunink MG, et al. Complex vascular anatomy in live kidney donation: imaging and consequences for clinical outcome. *Transplantation* 2008;85:1760-5.
  40. Neymark E, LaBerge JM, Hirose R, et al. Arteriographic detection of renovascular disease in potential renal donors: incidence and effect on donor surgery. *Radiology* 2000;214:755-60.
  41. Wu EH, Wojciechowski D, Chandran S, et al. Prevalence of abdominal aortic calcifications in older living renal donors and its effect on graft function and histology. *Transpl Int* 2015;28:1172-8.

42. Blondin D, Lanzman R, Schellhammer F, et al. Fibromuscular dysplasia in living renal donors: still a challenge to computed tomographic angiography. *Eur J Radiol* 2010;75:67-71.
43. Young JY, Ryu RK, Casalino DD. Fibromuscular dysplasia and renal transplantation. *J Urol* 2011;186:1073-4.
44. Rydberg J, Kopecky KK, Tann M, et al. Evaluation of prospective living renal donors for laparoscopic nephrectomy with multisection CT: the marriage of minimally invasive imaging with minimally invasive surgery. *Radiographics* 2001;21 Spec No:S223-36.
45. Arévalo Pérez J, Gragera Torres F, Marin Toribio A, et al. Angio CT assessment of anatomical variants in renal vasculature: its importance in the living donor. *Insights Imaging* 2013;4:199-211.
46. Pollak R, Prusak BF, Mozes MF. Anatomic abnormalities of cadaver kidneys procured for purposes of transplantation. *Am Surg* 1986;52:233-5.
47. Mandal AK, Cohen C, Montgomery RA, et al. Should the indications for laparoscopic live donor nephrectomy of the right kidney be the same as for the open procedure? Anomalous left renal vasculature is not a contraindication to laparoscopic left donor nephrectomy. *Transplantation* 2001;71:660-4.
48. Minnee RC, Bemelman WA, Maartense S, et al. Left or right kidney in hand-assisted donor nephrectomy? A randomized controlled trial. *Transplantation* 2008;85:203-8.
49. Martin G, Sundaram CP, Sharfuddin A, et al. Asymptomatic urolithiasis in living donor transplant kidneys: initial results. *Urology* 2007;70:2-5; discussion -6.
50. Harraz AM, Kamal AI, Shokeir AA. Urolithiasis in renal transplant donors and recipients: An update. *Int J Surg* 2016;36:693-7.
51. Olsburgh J, Thomas K, Wong K, et al. Incidental renal stones in potential live kidney donors: prevalence, assessment and donation, including role of ex vivo ureteroscopy. *BJU Int* 2013;111:784-92.
52. Sener A, Uberoi V, Bartlett ST, et al. Living-donor renal transplantation of grafts with incidental renal masses after ex-vivo partial nephrectomy. *BJU Int* 2009;104:1655-60.
53. Buell JF, Hanaway MJ, Thomas M, et al. Donor kidneys with small renal cell cancers: can they be transplanted? *Transplant Proc* 2005;37:581-2.

**Cite this article as:** Aghayev A, Gupta S, Dabiri BE, Steigner ML. Vascular imaging in renal donors. *Cardiovasc Diagn Ther* 2019;9(Suppl 1):S116-S130. doi: 10.21037/cdt.2018.11.02